Stand-alone lumbar cage subsidence: a biomechanical sensitivity study of cage design and placement.

Andrea Calvo-Echenique[1], José Cegoñino[1], Raúl Chueca[1], Amaya Pérez-del Palomar[1]

[1]Group of Biomaterials

Aragón Institute of Engineering Research (I3A)

Department of Mechanical Engineering, University of Zaragoza (Spain)

Corresponding author:

Amaya Pérez-del Palomar

María de Luna s/n

Departamento Ingeniería Mecánica, Ed. Betancourt, Escuela de Ingeniería y Arquitectura.

Zaragoza (Spain)

+34 976762872

amaya@unizar.es

Acknowledgments

This work was supported by the Spanish Ministry of Economy and Competitiveness through project DPI2016-79302-R and by the Spanish Ministry of Education, Culture and Sports (Grant FPU13/01070).

1. *Abstract and key terms*

Background and objective

Spinal degeneration and instability are commonly treated with interbody fusion cages either alone or supplemented with posterior instrumentation with the aim to immobilize the segment and restore intervertebral height. The purpose of this work is to establish a tool which may help to understand the effects of intervertebral cage design and placement on the biomechanical response of a patient-specific model to help reducing post-surgical complications such as subsidence and segment instability.

Methods

A 3D lumbar functional spinal unit (FSU) finite element model was created and a parametric model of an interbody cage was designed and introduced in the FSU. A Drucker-Prager cap plasticity formulation was used to predict plastic strains and bone failure in the vertebrae. The effect of varying cage size, cross-sectional area, apparent stiffness and positioning was evaluated under 500N preload followed by 7.5Nm multidirectional rotation and the results were compared with the intact model.

Results

The most influential cage parameters on the FSU were size, curvature congruence with the endplates and cage placement. Segmental stiffness was higher when increasing the cross-sectional cage area in all loading directions and when the cage was anteriorly placed in all directions but extension. In general, the facet joint forces were reduced by increasing segmental stiffness. However, these forces were higher than in the intact model in most of the cases due to the displacement of the instantaneous centre of rotation. The highest plastic deformations took place at the caudal vertebra under flexion and increased for cages with greater stiffness. Thus, wider cages and a more anteriorly placement would increase the volume of failed bone and, therefore, the risk of subsidence.

Conclusions

Cage geometry plays a crucial role in the success of lumbar surgery. General considerations such as larger cages may be applied as a guideline, but parameters such as curvature or cage placement should be determined for each specific patient. This model provides a proof-of-concept of a tool for the preoperative evaluation of lumbar surgical outcomes.

Key terms: Finite element model, stand-alone intervertebral cage, parametric model, subsidence, stability.

2. *Introduction*

Spinal degeneration and instability are commonly treated with interbody fusion cages either alone or supplemented with posterior instrumentation. The aim of this surgery is to stabilize the segment and restore intervertebral height. Lumbar cages are widely employed in combination with additional screw instrumentation to ensure segment immobilization and avoid the risk of non-union. However, although widely accepted as a successful treatment, this additional fixation, apart from being more invasive, has been reported to present some complications such as screw loosening or implant failure. Besides, some biomechanical studies have suggested that lumbar intervertebral disc (IVD) cages are sufficiently stable to be used as stand-alone devices [1], provided that they are introduced using a minimally invasive technique that ensures preservation of important stabilizing structures [2,3]. Large scale clinical studies have also demonstrated no differences in clinical outcomes between patients with stand-alone cages versus those with additional posterior fixation [4]. Although instability was initially defined as a loss of stiffness, and later as a reduction of the neutral zone [5], it is generally accepted that instability is associated with an abnormal load pattern which not necessarily would imply an increase in segmental movement as occurs during disc degeneration [6]. For that reason, and given that the fusion surgery aims to reduce the movement, throughout this paper the outcomes would be discuss in terms of segmental stiffness, directly related with the relative movement of the segment.

The use of stand-alone cages has shown to be very controversial presenting several problems chief of which is the risk of subsidence of the device into the bone owing to the high contact pressures on the bony endplates. For this reason, this study was focused on the investigation of possible factors which may contribute to reduce this risk in cages placed as a stand-alone construct. Although subsidence in early postoperative stage may increase the contact area, avoid the peak pressures caused by irregularities and prevent the progression of subsidence, high-grade subsidence can lead to a reduction in the intervertebral space height [7]. Thus, the use of an appropriate constitutive material of the vertebral bone incorporating a plasticity formulation would lead to a better prediction of the risk of subsidence in a stand-alone fashion. Previous studies have used Von Mises equivalent stress as the criterion for bone yielding [8,9]. However, considering that bone should be treated as a brittle material, the Von Mises criteria would not be suitable [10]. In this study, we used the modified Drucker–Prager Cap model, which takes the contribution of hydrostatic stress into consideration, as the yield criterion to model the inelastic behaviour at a continuum level.

On the other hand, cage characteristics such as shape, material and positioning are also expected to have a significant influence on surgery success. Previous studies have used finite element (FE) models to compare among commercial cages, but only some of them have discussed the influence of cage material [11] or shape [8,12] using parametric or optimization methods. In their study, Hsu et al.[12] used a genetic algorithm to find the cage shape with an optimal subsidence resistance. However, they assumed flat endplates instead of real geometry which may lead to a more uniform pressure distribution and an underestimation of subsidence risk. Later on, a study comparing a standard cage with a custom-fit one showed that patient-specific cage geometry could reduce the stress concentration on the endplates [8]. However, these studies provided a limited prediction of subsidence as they used elastic material models.

In this study we aimed to prove a model which will serve as a tool for the preclinical evaluation of surgery outcomes that any interbody device or supplementary fixation may have in each specific patient. Particularly, in this work, the influence of different design parameters and positioning of a bean-shaped cage on segment stiffness and subsidence risk has been studied. The selection of a stand-alone device responds to the higher risk of subsidence reported for this technique but in no case it is aimed to show a comparison with additional instrumentation or to demonstrate a superiority of one technique over the other. To this end, we conducted a parametric FE analysis of a cage design of varying size, cross-sectional area and position, and evaluated it in a patient-specific functional spinal unit (FSU). The main contribution of this study is the evaluation of cage subsidence with an elasto-plastic material formulation with different behaviour for traction and compression for the bone. In addition, this formulation accounted not only for the stresses over the yield stress limit, but also considered the hardening of the material.

3. *Materials and Methods*

A 3D FE model of a FSU was developed to evaluate the influence of cage design and positioning in the surgical outcome. Firstly, the intact segment was simulated and validated to set a control scenario. Then, the elements corresponding to the nucleus and inner annulus were removed to place a stand-alone cage. A total of 50 models were built (intact FSU + cage with neutral parameters + 8 variations of each parameter) as explained below.

FSU finite element model

A L4-L5 FSU was modelled including vertebral bodies, annulus fibrosus, nucleus pulposus, cartilaginous endplates, facet joints and the seven major ligaments. This model will be referred in the following as intact model. The vertebral bodies were segmented from a computed tomography of an asymptomatic 46-year-old male subject [13] and divided into a 0.5mm thick cortical layer [14] meshed with one layer of hexahedral elements and the cancellous bone, meshed with tetrahedral elements of 2mm mean size due to the geometrical irregularities. Bone was characterized as a transversal isotropic material with a Druker Prager cap plasticity formulation (see Online resource 1). Soft tissues were modelled according to anatomical characteristics: the annulus fibrosus and the endplates were meshed with linear hexahedral elements with mean mesh size of 1.5mm. For the annulus fibrosus (AF) an anisotropic material with two families of fibres (±30º), using the Holzapfel strain energy function, was used [13]. While, the endplates were characterized as linear elastic material. The nucleus pulposus was meshed with hexahedral elements and characterized as a non-linear NeoHookean material. The spinal ligaments were modelled as uniaxial truss elements with strain-dependent behaviour under traction and without resistance to compression. Finally, the facet joints were modelled as 0.2mm thickness cartilage with a frictionless surface-to-surface contact combined with a penalty algorithm for normal contact (200 N/m stiffness, initial gap of 0.4mm) [15]. All mechanical properties are summarized in Table I. To obtain the ideal size of the FE mesh (shown in Figure 1), a process of mesh refinement was executed until verifying mesh convergence. The mesh refinement process was stopped when the difference between the results was 5% or lower. This analysis gave a global mesh size which is summarized in Table II.

Cage design and parameterization

The intact model described previously was modified to introduce the cage. Thus, the elements corresponding to the nucleus pulposus and inner annulus were removed to host the cage. After the insertion, the empty region left between the annulus and the cage was filled with tetrahedral elements simulating the granulation or

129 inflammatory tissue (its mechanical properties are shown in Table I). Furthermore, simulating a minimally
130 invasive surgery, the ligaments were considered to remain intact.

131 A parametric model of a bean-shaped cage was created using Python scripting in ABAQUS 6.13 (SIMULIA,
132 Providence, RI, USA) (Figure 1a). The cross-sectional area of the cage was varied by modifying the axes
133 distance (length), radius (width) and thickness (Figure 1a) to investigate the influence of the apparent stiffness of
134 the cage. On the other hand, the curvature of the cage ends, which will contact the top and bottom vertebral
135 endplates, was varied from flat to high convexity to account for the effect of geometry congruence (Figure 1b).
136 This parameter was defined as the difference in percentage between the central and lateral cage height. An
137 additional transversal hole was included varying its height because, despite it is very common in commercial
138 cages to promote bone growth around the implant, it modifies the cage stiffness (Figure 1b). Finally, the cage
139 was placed at a central position and moved along the antero-posterior direction as shown in Figure 1c. The
140 election of the parameters to be varied responds to the clinically reported influence of cross-sectional area and
141 cage positioning on surgery outcome [7,16–18]. The neutral parameter values were set in accordance to the
142 standard shape of commercial implants. Then, one parameter was varied at a time while maintaining neutral
143 values for all other parameters. The upper and lower limits and the neutral values for each parameter are
144 summarized in Figure 1a, 1b and 1c. Each parameter has been varied uniformly between minimum and
145 maximum values with a total of 9 values per parameter. The cage was meshed with linear hexahedral elements
146 after a sensitivity mesh analysis (0.7mm size) and made of PEEK (Table I). A surface-to-surface contact with a
147 friction coefficient of 0.5 was assigned to the cage-endplate interface [18]. The penetration of the cage into the
148 granulation tissue was avoided with a normal non-penetrating contact.

149

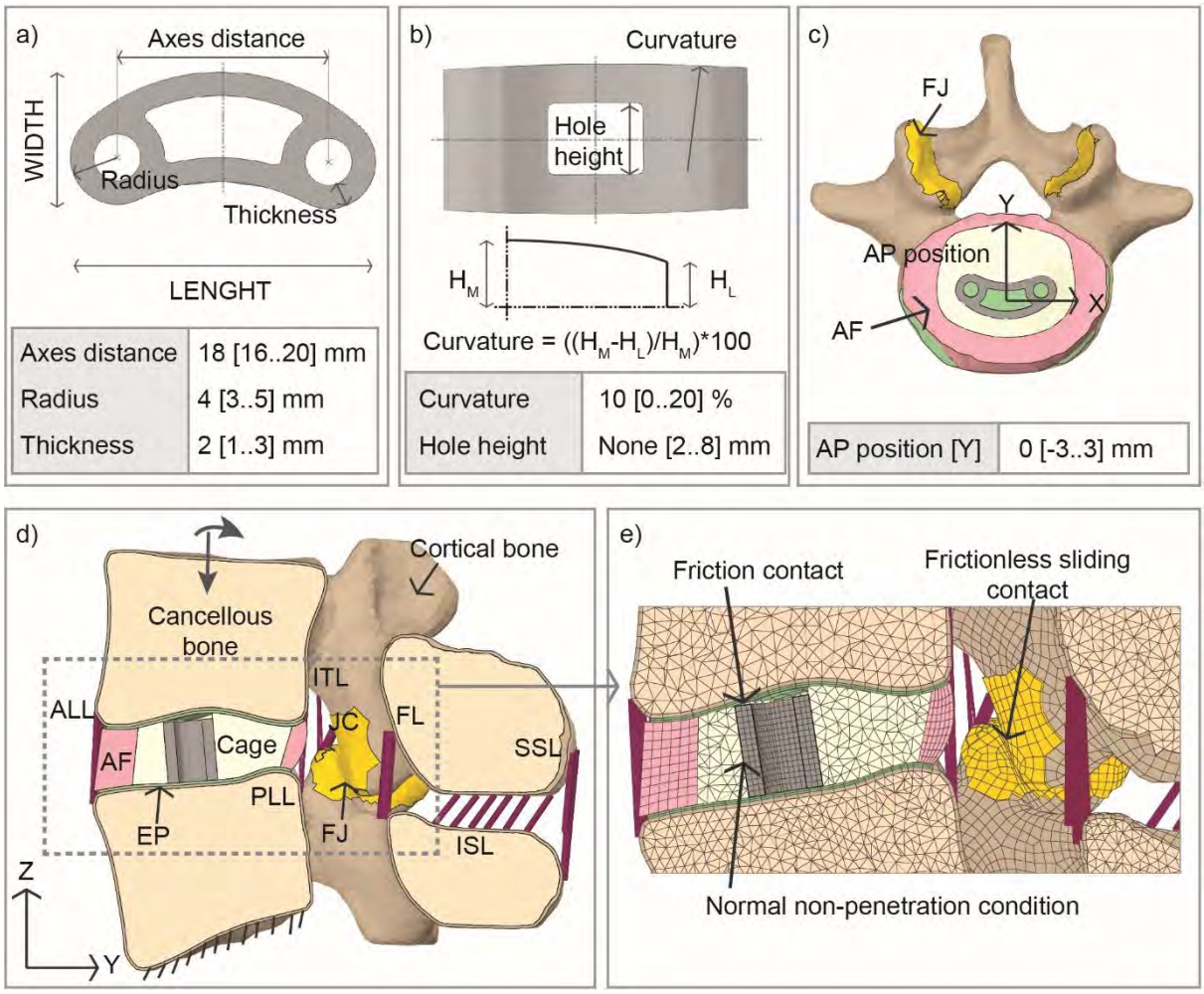

150

151 **Fig 1** a) Design parameters to vary the cross-sectional area of the cage; b) Design parameters to vary the
152 congruence of the ends in contact with the vertebrae (curvature), defined as the percentage of the difference
153 between the central (H_M) and the lateral (H_L) height of the cage, and a transversal hole (7mm width) with a
154 modifiable height; c) Cage placement on L5 vertebra, the cage was moved along the antero-posterior direction.
155 Granular tissue was considered between the annulus fibrosus (AF) and the cage. The facet joint (FJ) cartilage of
156 L5 is shown; d) FSU model including cortical and cancellous bone, endplates (EP), annulus fibrosus (AF),
157 ligaments [anterior longitudinal (ALL), intertransverse (ITL), posterior longitudinal (PLL), capsular (JC), flaval
158 (FL), interspinous (ISL) and supraspinous (SSL)], facet joints (FJ) and interbody cage. All movements were
159 constrained in the lower portion of L5 and the load was applied in the center of L4; e) Details of the mesh and
160 contact definitions of the FE model.

161

Table I. Material properties of the FSU components. ε_{12} defines the strain point at which the bi-linear elastic stress-strain curve change its slope from E_1 to E_2. *(PEEK-OPTIMA®, Invibio™ Biomaterials Solutions)

+Nucleus tissue only exists in the intact FSU model, while granular tissue is only present in the operated FSU.

	Young modulus [MPa]	Poisson coef.		Yield stress [MPa]	Ultimate yield strain [%]
Cortical bone [19,20]	$E_{XX} = E_{YY}$ =11300 E_{ZZ} = 22000 G_{XY} = 3800 $G_{YZ} = G_{XZ}$ = 5400	ν_{XY} = 0.0484 $\nu_{YZ} = \nu_{XZ}$ = 0.203	Tension Compression	155 173	-
Cancellous bone [19,21]	$E_{XX} = E_{YY}$ =140 E_{ZZ} = 200 $G_{XY} = G_{YZ} = G_{XZ}$ = 48.3	ν_{XY} = 0.045 $\nu_{YZ} = \nu_{XZ}$ = 0.315	Tension Compression	1.75 1.92	1.59 1.45
Endplates [19]	E = 23	ν = 0.4			
Facet joints [15]	E = 35	ν = 0.4			
Granular tissue [22]+	E =0.2	ν = 0.167			
Cage (PEEK)*	E = 4100	ν = 0.36		100-115	

	C_{10} [MPa]	D [MPa^{-1}]	K_1[MPa]	K_2
Annulus [23]	0.34	0.306	1.8	11
Nucleus [24]+	0.16	0.024	-	-

Ligaments [25,26]	E_1 [MPa]	E_2 [MPa]	ε_{12}	Number of elements	Area [mm^2]
ALL	7.8	20.0	0.12	10	32.9
PLL	1.0	2.0	0.11	9	5.2
LF	1.5	1.9	0.062	6	84.2
ITL	10.0	59.0	0.18	16	1.8
SSL	3.0	5.0	0.2	4	25.2

	Stiffness [N/mm]	ν	Number of elements	Area [mm^2]
JC	30.6 ± 1.5	0.4	14	43.8
ISL	8.7 ± 6.5	0.4	11	35.1

Table II. Mesh details. The granular and cage parts had different number of elements depending on the cage shape and are not listed within the table.

	ELEMENT TYPE	NUMBER OF NODES	NUMBER OF ELEMENTS
CORTICAL BONE	Hexahedral	32474	16432
CANCELLOUS BONE	Tetrahedral	63148	331542
ANNULUS FIBROSUS	Hexahedral	5216	4032
NUCLEUS PULPOSUS	Hexahedral	2664	2128
ENDPLATES	Hexahedral	5574	3520
FACET JOINTS	Squared membrane	921	817
LIGAMENTS	Truss	72	36

Boundary conditions

Firstly, the intact FSU was validated using previous in-vitro and computational studies [27,28]. Thus, a compressive load of 100N followed by a 7.5Nm moment in different directions was introduced and the obtained range of motion (ROM) was compared with the results available in the literature.

Afterwards, a physiological loading scenario was introduced. A compressive follower preload of 500N [29] was applied between the vertebral centres without any derived rotation. Then, a ±7.5Nm [30] moment load in flexion-extension, lateral bending and axial rotation at the centre of L4 was applied while movement at the lower portion of L5 was restricted. These conditions were applied to the intact FSU, as well as to the FSU with each cage design.

4. Results

Intact FSU validation

The ROM of the intact FSU was validated by comparison with in-vitro [27] and computational data [28] from literature. In Figure 2, the rotation of the intact FSU for every movement is compared with data in the literature, and a good result was achieved for every case. Notwithstanding the fact, that the variability obtained by Heuer and collaborators [27] is very high, our results also fall in the range of the computational analysis made by Zander and collaborators [28].

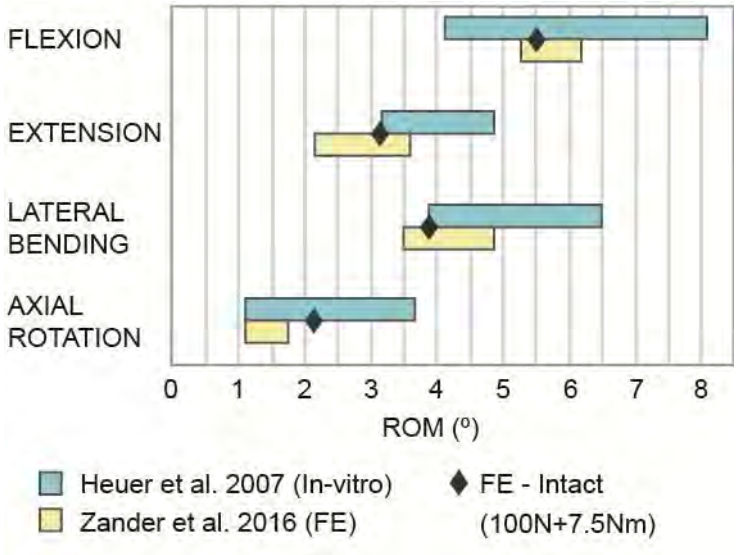

Fig 2. FSU ROM validation by comparison with previous in-vitro and computational models of L4-L5 segment.

Segmental stiffness

As it has been mentioned in the Introduction section, the segmental stiffness is directly related with the relative movement of the segment. For the same applied moment, an increase in the movement of the segment will imply a decrease in segmental stiffness. Thus, in this section, the ROM of the FSU for each cage design and position is compared with the rotation of the intact segment. In Figure 3, it can be seen that the parameters exerting the strongest effects were radius and antero-posterior position.

In this work it was assumed that a decrease in segmental stiffness with respect to the intact model would be undesirable for two reasons. Firstly because the aim of the surgery is to promote fusion with the consequent immobilization. And secondly, because an excessive motion could induce problems in the neighbouring structures. The segmental stiffness was increased by increasing the radius, which means a wider cage, in all loading directions. A longer cage, increasing the axes distance, led to a stiffer segment in extension and lateral bending while a higher curvature led to the opposite outcome. In addition, in axial rotation a flat cage reduced the segmental stiffness more than a biconvex one. On the other hand, the antero-posterior positioning of the cage had a different impact depending on the load direction: an anteriorly placed cage increased the segmental stiffness in flexion, lateral bending and axial rotation but decreased it in extension. However, an extreme posterior placement also increased the rotation in extension.

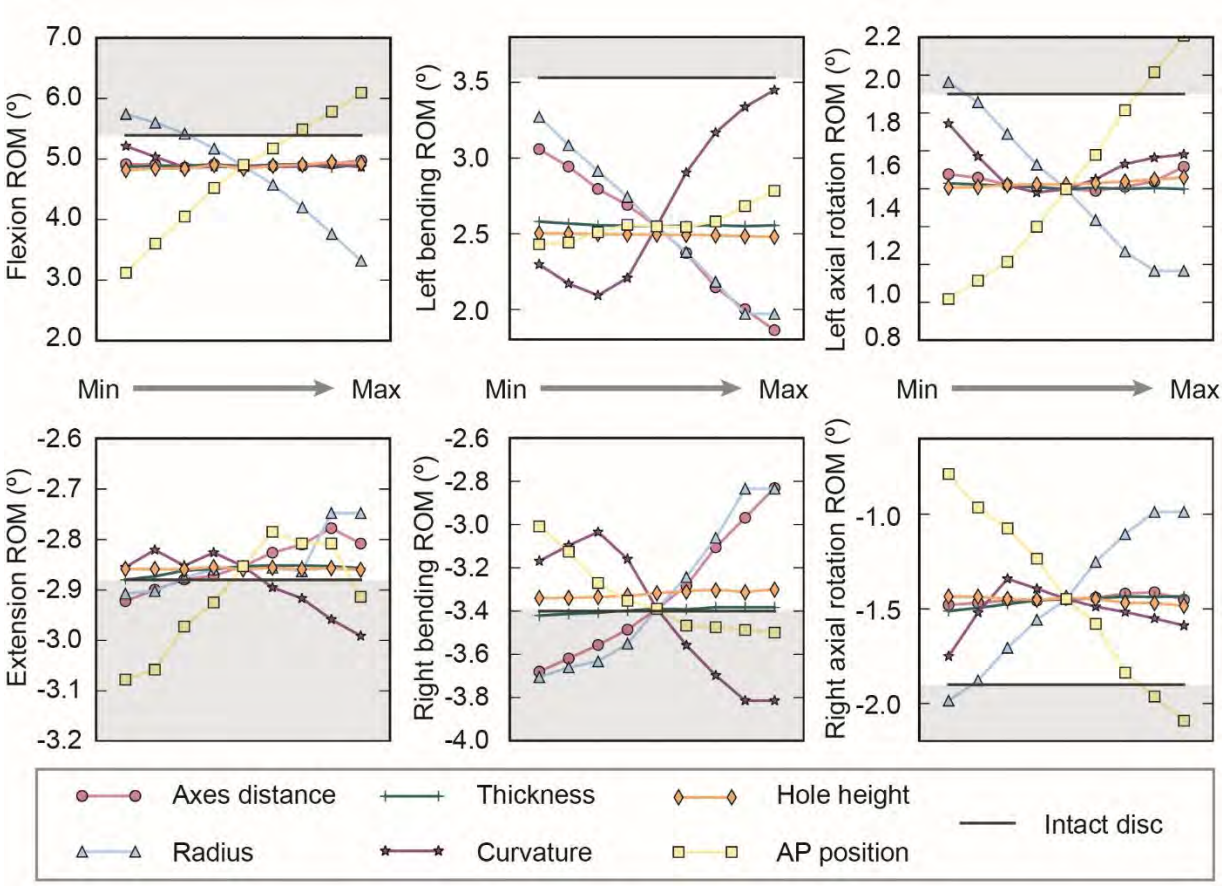

207

208 **Fig 3** Change of the final rotation of the FSU due to the variation of each parameter in flexion, extension, lateral
209 bending (LB) and axial rotation (AR). The rotation of the intact segment under the same conditions is shown as
210 reference. The shaded area denotes the ROM for which the segment would loss stiffness.

211 *Facet joint forces*

212 In flexion, the facet joints remained unloaded for the intact model. However, the presence of a cage led to the
213 appearance of facet forces, which were not significant in comparison with those depicted in Figure 4 for
214 extension, lateral bending, and axial rotation. As mentioned before, short cages and high curvatures caused an
215 increase of the segment movement increasing the facet forces more than 20% in extension and lateral bending,
216 and more than 30% in axial rotation. On the contrary, a drastic reduction of the facet forces was obtained when
217 the cage was posteriorly placed because most of the load was transmitted through the endplates instead of
218 through the posterior elements. Although in general, a higher segment stiffness was accompanied by a facet
219 force reduction, this force was in many cases higher than in the intact segment. This increment is related to the
220 displacement of the instantaneous centre of rotation (ICR).

221

222

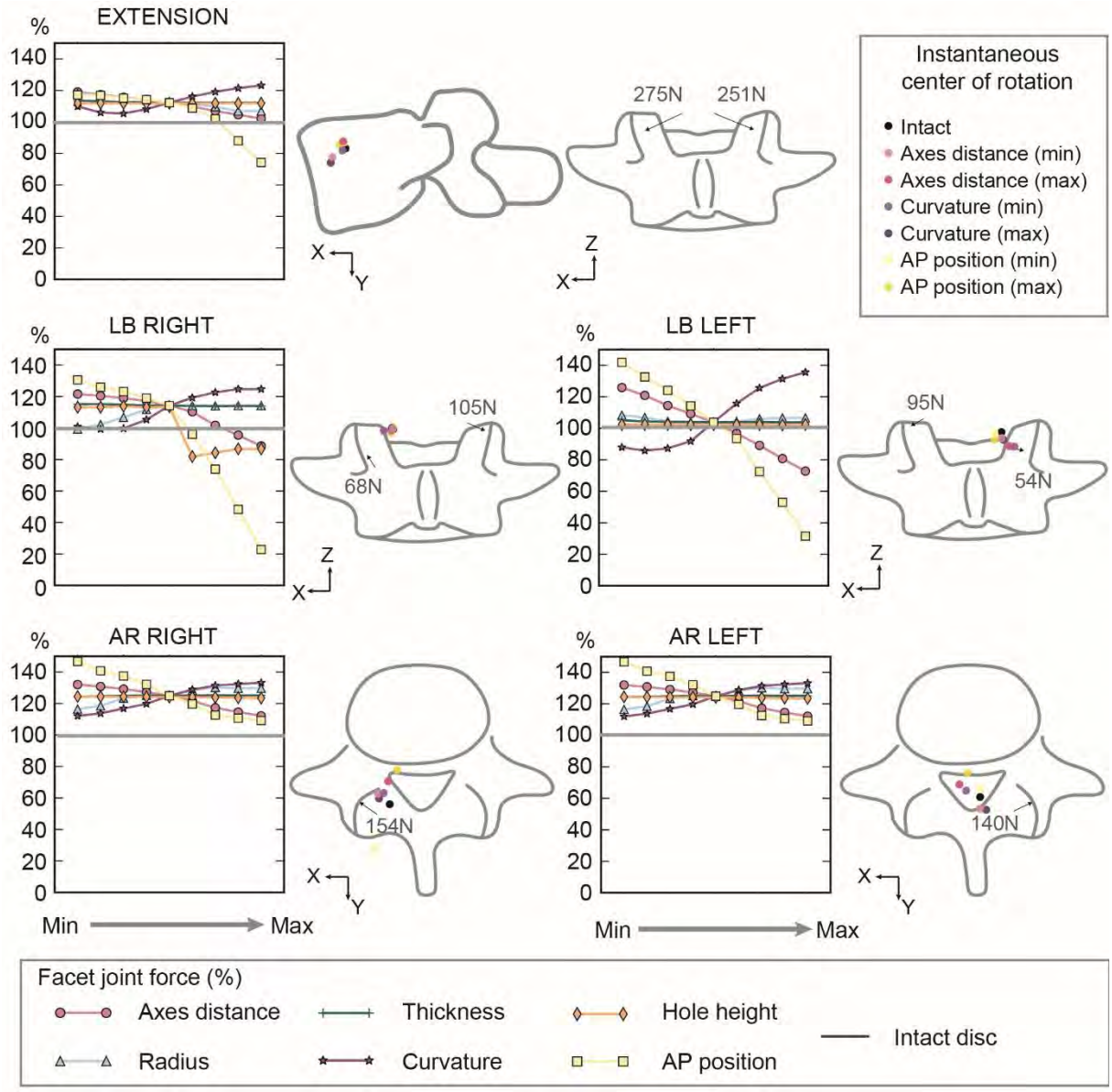

223

224 **Fig 4** Change in the force supported by the most loaded facet joint due to the variation of each parameter under
225 extension, lateral bending (LB) and axial rotation (AR) in percentage of the intact force. At the right of each
226 graph, the scheme of L5 has been depicted with the direction and value of the facet joint forces in the intact FSU.
227 The instantaneous center of rotation has been plotted for the intact case, and the maximum and minimum values
228 of the parameters which affect the most the facet joint forces (axes distance, curvature and AP position).

229

230 *Risk of cage subsidence*

231 After a careful analysis of the results, it was observed that the maximum contact pressures appeared for flexion
232 and lateral bending movements at the bottom endplate. Due to the irregularities of the endplate geometry, these

peak pressures took place on small areas and did not follow a uniform trend with the variations of the parameters. Therefore, the nominal contact pressures were analyzed. Once again, flexion and lateral bending transmitted the highest forces through the endplates and: radius, curvature and anteroposterior positioning, exerted the greatest influence. Regarding the bone integrity, it was observed that these parameters also had the greatest influence in the appearance of inelastic strains. Furthermore, caudal vertebra presented a higher volume of failed bone. Here the most significant results are shown; more details can be found in the Online resource 2. Figure 5 depicts the change in bone volume that had undergone inelastic strains with the most influential cage parameters. In flexion, it was observed that a cage with a curvature higher than 12.5% or a radius higher than 4.25mm caused bone failure preceding cage subsidence. In turn, an anteriorly placed cage also led to bone failure.

On the other hand, in extension, the yield zone moved backward to the vertebral arch and the facet joints, where the inelastic strains in the arch were primarily caused by tensile stresses due to the contact between the facet joints. Furthermore, plastic strains on the endplates were obtained with a posterior positioning of the cage.

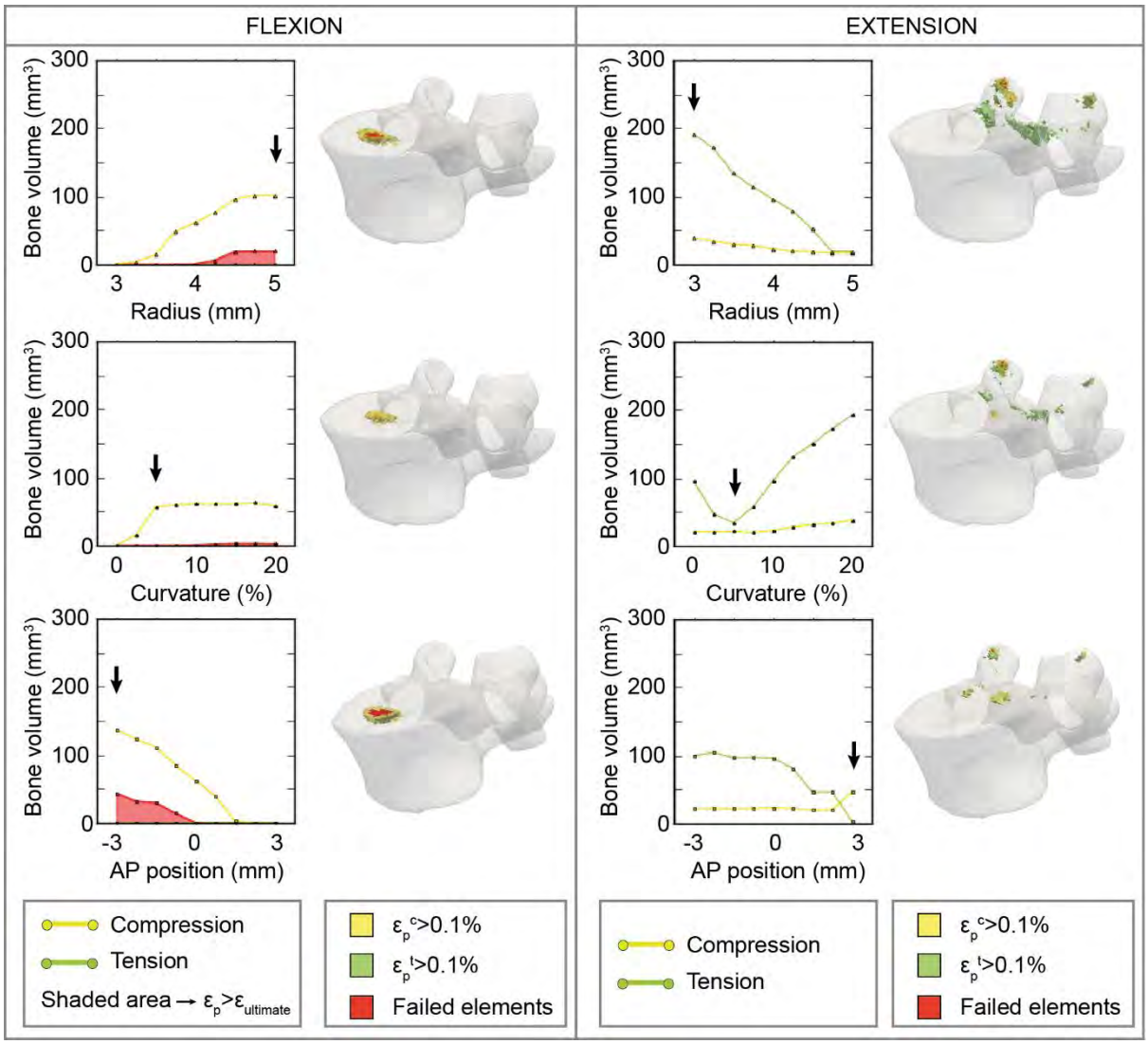

Fig 5 Change in the bone volume that undergone plastic strains due to the variation of radius, curvature and AP position. ε_p^c and ε_p^t are the plastic strains in compression and tension respectively (see Table I). The volume of failed bone has been represented as a shaded area. At the right of each graph, the distribution of plastic strain is shown in L5 for the case marked by the arrow.

5. *Discussion*

In this work, the effect of varying interbody cage design and placement on segmental stiffness and risk of subsidence has been studied using FE models with a post-yield characterization of the vertebral bone. Because the main goal of this work was to provide a useful tool for preoperative evaluation: range of motion, facet forces and bone integrity have been studied as key factors to achieve a successful fusion surgery.

Historically, supplementary fixation has proved to provide greater stability, however, recent clinical studies have shown successful fusion using stand-alone cages [2,4]. In this study, a stand-alone cage was tested using a patient specific geometry and the segmental stiffness based on the ROM was compared with an intact segment. Thus, higher segmental stiffness was predicted for wider and longer cages (high cross-sectional area) in agreement with in vitro and clinical findings [7,31]. Nonetheless, the maximum cage width would be ultimately determined by the risk of neural injury during the insertion. Cage placement has also demonstrated a high impact in segmental stiffness. As seen in clinical practice an anterior positioning of the cage makes for a stiffer construct [16]. In our study, all rotations were reduced when the cage was anteriorly placed except for extension movement. Similarly, previous studies reviewed elsewhere [32] have shown greater range of motion in extension. In these studies, the loss of stiffness may be caused by the removal of stabilizing structures such as ALL and facet joints while, here, these structures were preserved, simulating a minimally invasive surgery, and allowed to achieve a stiffer construct by varying the device design and placement.

Besides, an alteration in the load transmission through the posterior elements was observed with the variation of the interbody cage design. Our results showed that, the higher the segmental stiffness achieved, the less the forces at the facet joints, except for position variation. However, facet forces were higher than the intact ones for most of the analysed cases, which seems to be inconsistent with the idea of load sharing between posterior elements and a stiff interbody spacer. This inconsistency may be explained by the displacement of the ICR. In axial rotation, where the highest load increment was reported, the ICR moved towards the centre of the disc, changing the motion pathway of the upper vertebra and, therefore the contact through the facet joints. In fact, when the cage was posteriorly placed the facet forces significantly decreased in all movements because the load was mainly transmitted through the implant.

Finally, cage subsidence risk has been predicted based on contact pressures [11], Von Misses stresses [8] and total reaction force [12]. However, none of these outcomes account for bone failure which is the actual cause of subsidence. In our study, the maximum pressures were similar to those obtained previously [11], but a constant

trend was not found with the variation of the cage design parameters. The irregularities of the endplates naturally result in small contact areas with high loads, which may explain why the pressures did not show any trend when varying the design. Thus, they hindered the discussion of which parameters will enhance subsidence resistance. However, these pressures provoke stresses in the underlying bone which may cause inelastic strains.

To account for this inelastic behaviour, other authors used Von Mises equivalent stress as the criterion for bone yielding. However, considering that the tensile strength of bone is smaller than its compressive strength, bone should be treated as a brittle material and the Von Mises criteria would not be suitable [10]. Furthermore, compressing collapse of crushable bone cells allowed for a gradual decrease of the stresses and a local hardening of the tissue. This behaviour was studied by Kelly et al. [33] who proved that a crushable foam plasticity formulation with pressure dependent yield behaviour provided the best approximation to the stress-strain curve of the bone at a continuum level when compared with their results for a micro-FE model. Other studies [10,34] have also shown that the Druker-Prager formulation is able to predict the post-yield behaviour of the bone that can be improved by the definition of the hardening. In our model, the implementation of a modified Drucker-Prager Cap plasticity material behaviour allowed to predict bone failure and, therefore, cage subsidence. Contrary to other studies which found more inelastic strains in extension or lateral bending, in our model plastic strains were more prone to occur in the anterior part of the caudal vertebra during flexion. This difference may be related to the use of posterior fixation by Jalil et al. [35] which restricted the flexion motion decreasing the compressive force on the anterior part of the endplates. Regarding the cage parameters, the inelastic strains increased for cages with: high radius, high curvature and an anterior position. Thus, a wider cage reduced the range of motion at the same time that increased the risk of subsidence, and the same occurred with an anteriorly placed cage. So an equilibrium between segment stiffness and subsidence should be reached to determine the best cage design. In agreement with our results, previous FE studies showed that a higher cage stiffness would increase the risk of subsidence [11]. However, in contrast to our results, clinical studies have shown that a wider cage increases the subsidence resistance [7,36] because they lay in the peripheral region where the structural properties of the lumbosacral endplates are superior [37]. This disagreement is due to the fact that in this study uniform properties have been considered for the bony structures due to the lack of material data. Lastly, in extension, the yield zone moved backward to the vertebral arch and is mainly caused by tensile stresses. Here a constant cortical thickness was considered for the entire vertebra, however, the arch has actually a thicker cortical layer and, therefore, the stiffness of this part is higher and the inelastic strains would decrease.

It is noticeable that each cage design or positioning parameter was varied independently to determine those with a higher influence on the surgical outcome, rather than to find and optimal design. To look for the optimal cage, the interrelations would have to be taken into account and an optimization function would have to be defined considering the compromise between segmental stiffness and bone integrity.

This study has a number of limitations. Firstly, we used a high friction coefficient at the cage-endplate interface, assuming that the surfaces of the cages are prepared with a serrated geometry or roughness to avoid slippage of the device [38]. Nevertheless, this parameter would be more important for the risk of cage migration than for cage subsidence which is the goal of this work. Secondly, when modelling the mechanical behaviour of the cartilaginous endplates linear elasticity and constant thickness were assumed. Modelling using a hyperelastic material and irregular thickness would allow for a more accurate analysis of endplate behaviour. Regarding the facet joints, the properties were taken in accordance with other previous studies, however, slight changes in the gap distance, the degree of curvature or the facet orientation can lead to different results. In our study, the results have been normalized with the intact data for comparison. In the model, the cage insertion canal was not explicitly modelled. Given that the simulated surgery corresponded to a transforaminal lumbar interbody fusion (TLIF) approach an anterolateral annular defect should have being included for a more actual prediction. However, although it is expected to cause some asymmetry in the results, the largest part of the load was transmitted through the cage and the posterior elements so it was assumed that the difference would not be significant. Furthermore, the distraction of the segment due to the cage press-fit was not included. If the cage height would be higher than the initial disc height, all the surrounding structures such as ligaments, muscles and annular fibres would present a pre-strain which would increase the load in the cage and, therefore, the contact pressures on the endplates. Nevertheless, considering that this pre-strain would affect all the cases, the predicted trends with varying parameters is expected to be unaltered. For a more deep understanding of the effect of segment distraction, a further parametric study should be performed varying cage height, and also considering that the segment would adapt to the cage differently in each position depending on the specific geometry, so that the pre-strain state of each structure would change from one to another. Furthermore, subsidence is directly related to bone quality which must be cautiously evaluated preoperatively. In this model, the material properties chosen for bone modelling corresponded with the lowest ones found in the literature [21] to create the worst possible scenario. Moreover, they were considered uniform along the bony endplates. A characterization of the local thickness and bone mineral density of the cortical and cancellous bone, derived from CT images via Hounsfield unit translation into bone mineral density, would improve the subsidence prediction. Besides, as was

shown in other studies [39] the vertebral endplate morphology follows the bone remodelling principles. When an implant is placed, the load sharing among the different regions of the endplate modified the mechanical environment of the bone forming cells initiating a remodelling process which may lead to a new situation. In further studies, the adaptive bone response to mechanical alterations should be studied in combination with its inelastic behaviour. Finally, a quasistatic load was applied to cross compare among implants while the physiologic environment of the lumbar segment would be better reproduced by a cyclic loading. It is expected that the elements which underwent inelastic strains accumulate damage over time driving to the progressive sinking of the implant into the vertebral body. Nevertheless, this study aims for the comparison between cage designs, so it is expected that the higher the inelastic strains in the static case, the higher the accumulated damage during time.

This model goes a step forward in subsidence prediction with the possibility to discern if the bone will fail under the cage pressure or not. It was seen that cage design and placement played an important role in the biomechanical behaviour of the FSU after lumbar surgery. A compromise between segment stiffness and bone integrity should be reached by modifying the cross-sectional area, geometrical congruence and position of the cage for each specific patient and each particular instrumentation. For that purpose, the model presented above may be a useful tool for the preoperative evaluation of patient-specific surgery outcome. Having medical images from the patient, it would be possible to segment the specific geometry and translate the Hounsfield units into bone density information, allowing to test different instrumentations for this specific patient following the same rationale. However, there are still aspects that should be included in order to construct accurate patient specific models. For instance, the estimation of real muscle forces using optimization principles based on the range of motion of that specific patient. Future researches could approach these issues.

Conflict of interest statement

The authors have not conflict of interest to declare.

6. References

[1] T.A. Zdeblick, F.M. Phillips, Interbody cage devices., Spine (Phila. Pa. 1976). 28 (2003) S2–7. doi:10.1097/01.BRS.0000076841.93570.78.

[2] A. Ahmadian, K. Bach, B. Bolinger, G.M. Malham, D.O. Okonkwo, A.S. Kanter, J.S. Uribe, Stand-alone minimally invasive lateral lumbar interbody fusion: Multicenter clinical outcomes, J. Clin. Neurosci. 22 (2015) 740–746. doi:10.1016/j.jocn.2014.08.036.

[3] F. Costa, M. Sassi, A. Ortolina, A. Cardia, R. Assietti, A. Zerbi, M. Lorenzetti, F. Galbusera, M. Fornari, Stand-alone cage for posterior lumbar interbody fusion in the treatment of high-degree degenerative disc disease: Design of a new device for an "old" technique. a prospective study on a series of 116 patients, Eur. Spine J. 20 (2011) 46–56. doi:10.1007/s00586-011-1755-0.

[4] E. Van de Kelft, J. Van Goethem, Trabecular metal spacers as standalone or with pedicle screw augmentation, in posterior lumbar interbody fusion: a prospective, randomized controlled trial, Eur. Spine J. 24 (2015) 2597–2606. doi:10.1007/s00586-015-4229-y.

[5] M. Panjabi, The stabilizing system of the spine. Part II. Neutral zone and instability hypothesis., J. Spinal Disord. 5 (1992) 390–397.

[6] R.C. Mulholland, The myth of lumbar instability: The importance of abnormal loading as a cause of low back pain, Eur. Spine J. 17 (2008) 619–625. doi:10.1007/s00586-008-0612-2.

[7] L. Marchi, N. Abdala, L. Oliveira, R. Amaral, E. Coutinho, L. Pimenta, Radiographic and clinical evaluation of cage subsidence after stand-alone lateral interbody fusion., J. Neurosurg. Spine. 19 (2013) 110–1188. doi:10.3171/2013.4.SPINE12319.

[8] L.S. Chatham, V. V. Patel, C.M. Yakacki, R.D. Carpenter, Interbody Spacer Material Properties and Design Conformity for Reducing Subsidence During Lumbar Interbody Fusion, J. Biomech. Eng. 139 (2017) 1–8. doi:10.1115/1.4036312.

[9] X. Liu, J. Ma, P. Park, X. Huang, N. Xie, X. Ye, Biomechanical comparison of multilevel lateral interbody fusion with and without supplementary instrumentation: a three-dimensional finite element study, BMC Musculoskelet. Disord. 18 (2017) 63. doi:10.1186/s12891-017-1387-6.

[10] M. Bessho, I. Ohnishi, J. Matsuyama, T. Matsumoto, K. Imai, K. Nakamura, Prediction of strength and strain of the proximal femur by a CT-based finite element method, J. Biomech. 40 (2007) 1745–1753.

doi:10.1016/j.jbiomech.2006.08.003.

[11] F. Galbusera, H. Schmidt, H.-J.J. Wilke, Lumbar interbody fusion: A parametric investigation of a novel cage design with and without posterior instrumentation, Eur. Spine J. 21 (2012) 455–462. doi:10.1007/s00586-011-2014-0.

[12] C.C. Hsu, Shape optimization for the subsidence resistance of an interbody device using simulation-based genetic algorithms and experimental validation, J. Orthop. Res. 31 (2013) 1158–1163. doi:10.1002/jor.22317.

[13] J. Cegoñino, V. Moramarco, A. Calvo-Echenique, C. Pappalettere, A. Pérez Del Palomar, A constitutive model for the annulus of human intervertebral disc (IVD): implications for developing a degeneration model and its influence on lumbar spine functioning, J. Appl. Math. 2014 (2014). doi:10.1155/2014/658719.

[14] M. Silva, C. Wang, T. Keaveny, H. WC, Direct and computed tomography thickness measurements of the human, lumbar vertebral shell and endplate., Bone. 15 (1994) 409–414.

[15] H. Schmidt, F. Galbusera, A. Rohlmann, T. Zander, H.J. Wilke, Effect of multilevel lumbar disc arthroplasty on spine kinematics and facet joint loads in flexion and extension: A finite element analysis, Eur. Spine J. 21 (2012) S663–S674. doi:10.1007/s00586-010-1382-1.

[16] A. Castellvi, S. Thampi, D. Cook, M. Yeager, Y. Yao, Q. Zou, D. Whiting, M. Oh, E. Prostko, B. Cheng, Effect of TLIF Cage Placement on In Vivo Kinematics, Int. J. Spine Surg. (2015) 1–7. doi:10.14444/2038.

[17] A. Abbushi, M. Cabraja, U.W. Thomale, C. Woiciechowsky, S.N. Kroppenstedt, The influence of cage positioning and cage type on cage migration and fusion rates in patients with monosegmental posterior lumbar interbody fusion and posterior fixation, Eur. Spine J. 18 (2009) 1621–1628. doi:10.1007/s00586-009-1036-3.

[18] S. Vadapalli, K. Sairyo, V.K. Goel, M. Robon, A. Biyani, A. Khandha, N. a Ebraheim, Biomechanical rationale for using polyetheretherketone (PEEK) spacers for lumbar interbody fusion-A finite element study., Spine (Phila. Pa. 1976). 31 (2006) E992–E998. doi:10.1097/01.brs.0000250177.84168.ba.

[19] Y.M. Lu, W.C. Hutton, V.M. Gharpuray, Can variations in intervertebral disc height affect the mechanical function of the disc?, Spine (Phila. Pa. 1976). 21 (1996) 2208–2217. doi:10.1097/00007632-

199610010-00007.

[20] Y. Kim, Finite element analysis of anterior lumbar interbody fusion: threaded cylindrical cage and pedicle screw fixation., Spine (Phila. Pa. 1976). 32 (2007) 2558–68. doi:10.1097/BRS.0b013e318158cdd8.

[21] D.L. Kopperdahl, T.M. Keaveny, Yield strain behavior of trabecular bone, J. Biomech. 31 (1998) 601–608. doi:10.1016/S0021-9290(98)00057-8.

[22] D. Lacroix, P.J. Prendergast, A mechano-regulation model for tissue differentiation during fracture healing: Analysis of gap size and loading, J. Biomech. 35 (2002) 1163–1171. doi:10.1016/S0021-9290(02)00086-6.

[23] R. Eberlein, G. a. Holzapfel, C. a. J. Schulze-Bauer, An Anisotropic Model for Annulus Tissue and Enhanced Finite Element Analyses of Intact Lumbar Disc Bodies, Comput. Methods Biomech. Biomed. Engin. 4 (2001) 209–229. doi:10.1080/10255840108908005.

[24] V. Moramarco, A. Pérez del Palomar, C. Pappalettere, M. Doblaré, An accurate validation of a computational model of a human lumbosacral segment, J. Biomech. 43 (2010) 334–342. doi:10.1016/j.jbiomech.2009.07.042.

[25] J. Chazal, A. Tanguy, M. Bourges, G. Gaurel, G. Escande, M. Guillot, G. Vanneuville, Biomechanical properties of spinal ligaments and a histological study of the supraspinal ligament in traction, J. Biomech. 18 (1985) 167–176. doi:10.1016/0021-9290(85)90202-7.

[26] F. Pintar, N. Yoganandan, T. Myers, Biomechanical properties of human lumbar spine ligaments, J. Biomech. 25 (1992) 1351–1356.

[27] F. Heuer, H. Schmidt, Z. Klezl, L. Claes, H.-J. Wilke, Stepwise reduction of functional spinal structures increase range of motion and change lordosis angle, J. Biomech. 40 (2007) 271–280. doi:10.1016/j.jbiomech.2006.01.007.

[28] T. Zander, M. Dreischarf, A.-K. Timm, W.W. Baumann, H. Schmidt, Impact of material and morphological parameters on the mechanical response of the lumbar spine — A finite element sensitivity study, J. Biomech. 53 (2016) 185–190. doi:10.1016/j.jbiomech.2016.12.014.

[29] V. Goel, M. Panjabi, A. Patwardhan, A. Dooris, H. Serhan, A.S. for T. and Materials, Test protocols for evaluation of spinal implants, J. Bone Jt. Surg. Am. 88 (2006) 103–109. doi:10.2106/JBJS.E.01363.

[30] H.J. Wilke, K. Wenger, L. Claes, Testing criteria for spinal implants: recommendations for the standarization of in vitro stability testing of spinal implants., Eur. Spine J. 7 (1998) 148–154.

[31] L. Pimenta, A.W.L. Turner, Z. a Dooley, R.D. Parikh, M.D. Peterson, Biomechanics of lateral interbody spacers: going wider for going stiffer., Sci. World J. 2012 (2012) 6. doi:10.1100/2012/381814.

[32] T. Oxland, T. Lund, Biomechanics of stand-alone cages and cages in combination with posterior fixation: a literature review, Eur. Spine J. 9 (2000) S095–S101.

[33] N. Kelly, N.M. Harrison, P. McDonnell, J.P. McGarry, An experimental and computational investigation of the post-yield behaviour of trabecular bone during vertebral device subsidence, Biomech. Model. Mechanobiol. 12 (2013) 685–703. doi:10.1007/s10237-012-0434-3.

[34] A. Phillips, P. Pankaj, F. May, K. Taylor, C. Howie, A. Usmani, Constitutive models for impacted morsellised cortico-cancellous bone, Biomaterials. 27 (2006) 2162–2170. doi:10.1016/j.biomaterials.2005.10.034.

[35] M.H. Jalil, M.H. Mazlan, M. Todo, Biomechanical Comparison of Polymeric Spinal Cages Using Ct Based Finite Element Method, Int. J. Biosci. Biochem. Bioinforma. 7 (2017) 110–117. doi:10.17706/ijbbb.2017.7.2.110-117.

[36] T. V Le, A. a. Baaj, E. Dakwar, C.J. Burkett, G. Murray, D. a. Smith, J.S. Uribe, Subsidence of Polyetheretherketone Intervertebral Cages in Minimally Invasive Lateral Retroperitoneal Transpsoas Lumbar Interbody Fusion, Spine (Phila. Pa. 1976). 37 (2012) 1268–1273. doi:10.1097/BRS.0b013e3182458b2f.

[37] T.G. Lowe, S. Hashim, L. a Wilson, M.F. O'Brien, D. a B. Smith, M.J. Diekmann, J. Trommeter, A biomechanical study of regional endplate strength and cage morphology as it relates to structural interbody support., Spine (Phila. Pa. 1976). 29 (2004) 2389–2394. doi:10.1097/01.brs.0000143623.18098.e5.

[38] S.-H. Chen, C.-L. Tai, C.-Y. Lin, P.-H. Hsieh, W.-P. Chen, Biomechanical comparison of a new stand-alone anterior lumbar interbody fusion cage with established fixation techniques - a three-dimensional finite element analysis., BMC Musculoskelet. Disord. 9 (2008). doi:10.1186/1471-2474-9-88.

[39] A. Agarwal, A.K. Agarwal, V.K. Goel, The Endplate Morphology Changes with Change in Biomechanical Environment Following Discectomy, Int. J. Clin. Med. 04 (2013) 8–17.

481 doi:10.4236/ijcm.2013.47A1002.

482

483